Artifact or Architecture? An Integrated Approach to Visualizing Uncertainty and Partial Volume Effects in DT-MRI Tractography

D. K. Jones[1,2], A. R. Travis[3], G. M. Eden[4], C. Pierpaoli[1], P. J. Basser[1]

[1]STBB / LIMB, NICHD, National Institutes of Health, Bethesda, MD, United States, [2]Institute of Psychiatry, London, United Kingdom, [3]Biomedical Engineering, Vanderbilt University, Nashville, TN, United States, [4]Science, Mathematics and Computer Science Magnet Program, Montgomery Blair High School, Silver Spring, MD, United States

Introduction: DT-MRI tractography is receiving increasing attention in the neuroscience and neurosurgical communities for its potential to reconstruct white matter fasciculi non-invasively. However, while the *trajectories* of fasciculi have been visualized, other tract-specific features (including uncertainty in fiber orientation or partial volume artifacts) have not. Here we describe an integrated approach for visualizing these local tract characteristics *in situ*, which relies on the bootstrap method and *hyper*-streamline visualization. This allows one to assess whether the tract is passing near a region of CSF or gray matter or through a region in which fiber architecture is complex. It can help one decide whether the tractography results are artifact or architecture.

Method: Whole brain DT-MRI data (1.7 mm isotropic resolution, 84 contiguous slices) were acquired from healthy volunteers using 16 repeat samples of the 7 diffusion-weighted images (DWIs) acquired using the dual-gradient scheme[1], (i.e. 0, +*xy*, -*xy*, +*xz*, -*xz*, +*yz*, -*yz*). Following distortion / motion correction, the diffusion tensor was computed in each voxel from the set of 112 DWIs acquired at each slice location (dubbed the 'superset'). Tracts were launched from seedpoints using a *continuous* tensor field representation and tractography algorithm similar to that described elsewhere[2]. At each trajectory vertex, various indices of diffusion were computed including Trace, fractional anisotropy (*FA*), and the "Westin measures"[3] of tensor linearity (C_l), planarity (C_p) and sphericity (C_s). Furthermore, the 95% cone of uncertainty (95% CU) in fiber orientation was computed at each vertex using an approach similar to Jones[4], but assuming each bootstrap experiment consists of 42 images (i.e. 6 × 7 unique DW images). For each bootstrapped DT-MRI volume, fiber tracking was performed to generate 1000 estimates of tract trajectories from each seedpoint. The various indices (e.g. Trace, *FA*, C_p, C_l, C_s, 95% CU) were then visualized by appropriately coloring the facets of the streamtube at each vertex and/or by creating a hyperstreamline[5] (i.e. a streamtube that follows the principal eigenvector, but whose width varies in proportion to the measure of interest). We also developed a graphical user interface (GUI) to visualize all indices simultaneously as a function of arc length for each tract.

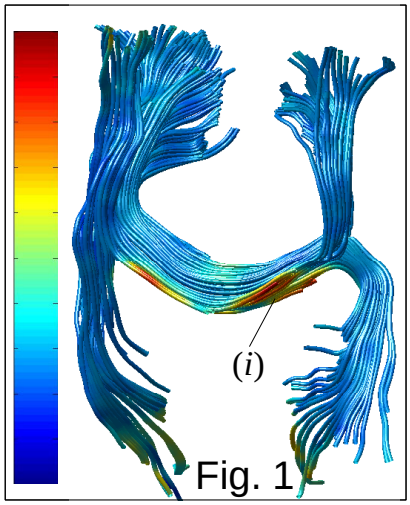

Fig. 1

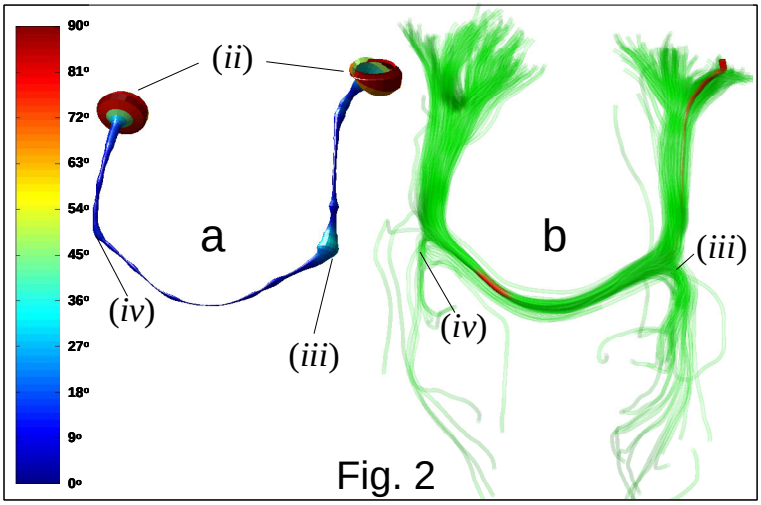

Fig. 2

Results: Fig. 1 shows streamtubes in the body of the corpus callosum and internal capsule, which are color-encoded for Trace. While the trace is fairly uniform throughout most of the tracts, at point (*i*) the trace is elevated where tracts pass close to the lateral ventricles, suggesting some partial volume contamination with CSF. Similar (although less marked) effects are observed as the tracts near the cortex. Fig. 2a shows the hyperstreamline encoded by the 95% cone of uncertainty for a tract reconstructed from a single seed point, while Fig. 2b shows the bootstrapped trajectories for this tract (green translucent tubes) together with the trajectory computed from the 'superset' (red tube). At (*iii*) in Fig. 2a, the hyperstreamline flairs out – which is reflected by a large number of bootstrapped tracts projecting away from the superset trajectory. At (*iv*), the hyperstreamline flairs to a lesser extent and, likewise, fewer bootstrapped tracts deviate away from the superset trajectory than at (*iii*). The hyperstreamline visualization in Fig. 2a provides a more succinct and readily interpreted visualization than Fig. 2b.

Discussion: While DT-MRI tractography can undoubtedly provide tract reconstructions that appear anatomically faithful, tract visualizations have so far been limited just to the course of the fasciculus of interest. Color-encoded streamtubes and / or hyperstreamlines provide a rich tract visualization that allows one to assess diffusion indices, partial volume effects, and uncertainty in fiber orientation at each point along a pathway. Simultaneously plotting all indices (Trace, *FA*, *Cp*, *Cl*, *Cs*, 95% CU) as a function of arc length (not shown) provides a deeper understanding of the various pathologies inherent in tractography and their effects. For example, a region with abnormally high trace (3.98×10^{-3} mm^2 s^{-1} – indicative indicative of partial volume contamination with CSF), low *FA* (0.229) and comparable values of C_p (0.119) and C_l (0.095), had only a slight increase in the 95% CU (19º) compared with the average 95% CU (≈ 12°). In contrast, in a nearby region in which the trace was normal In contrast, in a nearby region in which the trace was normal (2.1×10^{-3} mm^2 s^{-1}), *FA* was low (0.242), but C_p (0.274) was substantially higher than C_l (0.010), the 95% CU was substantially larger (85°). Here DT-MRI tractography provides tract reconstructions that appear anatomically faithful, but may be artifactual.

Conclusion: We have described an integrated approach for visualizing a number of diffusion indices together with the actual probability density function in fiber orientation in tandem with the course of white matter trajectories. This approach assists in identifying pathologies that would otherwise remain hidden in 'trajectory only' visualizations and will improve the interpretability of DT-MRI tractography results, helping to prevent the observer from mistaking artifact from architecture.

References: 1. Pierpaoli C *et al. Radiology* 1996; 201: 637-648; Basser PJ *et al. Magn Reson Med* 2000; 44: 625-632; **2.** Westin C-F *et al.* Proc ISMRM 1997, p. 1742. **3.** Jones DK. *Magn Reson Med* 2003; 49: 7-12; **4.** Delmarcelle T and Hesselink L. *IEEE Comp Graph* 1993; 13: 25-33.